Journal of Inflammation Research

Dovepress
open access to scientific and medical research

Open Access Full Text Article

ORIGINAL RESEARCH

Vitamin D Ameliorates Apoptosis and Inflammation by Targeting the Mitochondrial and MEK1/2-ERK1/2 Pathways in Hyperoxia-Induced Bronchopulmonary Dysplasia

Jinhui Hu[1,2,*], Zhixin Wu[1,*], Huawei Wang[1], Haifeng Geng[1], Jie Huo[1,3], Xueping Zhu[1], Xiaoli Zhu[4]

[1]Department of Neonatology, Children's Hospital of Soochow University, Suzhou, People's Republic of China; [2]Neonatal Medical Center, Huai'an Maternity and Child Health Care Hospital, Xuzhou Medical University, Huai'an, People's Republic of China; [3]Department of Neonatology, Yangzhou Maternity and Child Health Care Hospital, Yangzhou, People's Republic of China; [4]Department of Intervention, The First Affiliated Hospital of Soochow University, Suzhou, People's Republic of China

*These authors contributed equally to this work

Correspondence: Xueping Zhu, Department of Neonatology, Children's Hospital of Soochow University, No. 92 Zhongnan Street, Industrial Park, Suzhou, Jiangsu, 215025, People's Republic of China, Tel +86-13073304816, Fax +86-512-80693599, Email zhuxueping4637@hotmail.com; Xiaoli Zhu, Department of Intervention, The First Affiliated Hospital of Soochow University, 899 Pinghai Road, Gusu District, Suzhou, Jiangsu, 215006, People's Republic of China, Tel +86-13013805898, Fax +86-512-65233905, Email zhuxiaoli90@hotmail.com

Purpose: Bronchopulmonary dysplasia (BPD) is a common and severe complication in preterm infants. Vitamin D (VitD) has been reported to protect against BPD; however, its role in the mitochondria-mediated and MEK1/2-ERK1/2 pathways has not yet been reported.

Methods: We first performed in vivo studies using neonatal C57BL/6 mice in which we induced BPD by exposing them to a hyperoxic environment (85% O_2). The mice were divided into room air (RA; 21% O_2), RA+VitD, BPD, and BPD+VitD groups. Hematoxylin and eosin and Masson's trichrome staining were used to evaluate lung injury. Inflammation and apoptosis were measured using ELISA, RT-qPCR, and TUNEL assays. We then analyzed BEAS-2B cells divided into the same groups along with an additional BPD+VitD+inhibitor group. Mitochondrial apoptosis was evaluated by transmission electron microscopy, mitochondrial membrane potential, and Western blotting. We then used VDR-shRNA to silence the Vitamin D Receptor (VDR) in the BEAS-2B cells. The inflammation, apoptotic rate, and the phosphorylated forms of MEK1/2 and ERK1/2 in cells were detected by RT-qPCR, flow cytometry, and Western blotting.

Results: The mean linear intercept, septal thickness, and abnormal fibrosis increased, while radial alveolar count decreased in BPD lungs compared to RA lungs. VitD administration was able to ameliorate the phenotype in BPD lungs. IL-6, IFN-γ, and TNF-α expression and the apoptotic rate decreased in the BPD+VitD lung group. VitD pretreatment restored abnormal mitochondrial morphology, reduced mitochondrial membrane loss, and reduced the expression of cleaved caspase-3, Bax, and Bcl-2 in BEAS-2B cells. VitD administration also reduced IL-6, IFN-γ, and TNF-α mRNA, as well as pMEK1/2 and pERK1/2 expression and apoptosis rate in cells exposed to hyperoxia.

Conclusion: We concluded that VitD treatment ameliorated apoptosis and inflammation by targeting the mitochondrial pathway and via the MEK1/2-ERK1/2 signaling pathway in BPD, thus supporting its potential therapeutic use in this condition.

Keywords: bronchopulmonary dysplasia, vitamin D, hyperoxia, apoptosis, inflammation, mitochondria, MEK1/2-ERK1/2

Introduction

Bronchopulmonary dysplasia (BPD) is a common and severe complication in preterm infants. Over the past few years, the incidence of BPD has increased due to the improved survival from extremely preterm birth.[1] Patients with BPD often have poor outcomes that persist into adulthood. Despite its adverse long-term impact on respiratory function, BPD currently has no effective treatment option due to its interactive mechanisms with multifactorial etiology including

Received: 22 April 2022
Accepted: 16 August 2022
Published: 25 August 2022

hyperoxia and inflammation. Therefore, there is an urgent need to study the BPD pathogenesis and identify potential therapeutic opportunities with newer pharmacological approaches.

Vitamin D (VitD) has multiple biological effects on calcium homeostasis and metabolism.[2] Recently, VitD has been recognized as having a role in other processes, such as cell proliferation and anti-inflammatory activities.[3,4] Another study revealed that some chronic lung diseases are accompanied by VitD deficiency.[5] Furthermore, individuals who suffered preterm birth were more susceptible to VitD deficiency and BPD than full-term infants.[6] VitD has been shown to relieve pulmonary injury, inflammation, and apoptosis in a hyperoxia-induced mouse model.[7,8] Finally, preclinical studies of BPD have shown that VitD has potential effects on lung development as it regulates cell growth and apoptosis.[9,10]

The mitogen-activated protein kinase (MAPK) pathway involves MEK1/2 and ERK1/2 kinases, which regulate cell proliferation, inflammation, and apoptosis, and activation of the pathway by phosphorylation of key targets is known to play a crucial role in cancer.[11,12] Many growth factors trigger the activation of the MEK1/2-ERK1/2 signaling pathway, and the upregulation of phosphorylated forms has been detected in many solid tumors and lung diseases.[13] A recent study revealed that phosphorylated MEK1/2 and ERK1/2 expression increased in the lungs of an experimental acute lung injury model.[14]

There is a growing recognition that inflammation critically impacts BPD progression and severity, and that chorioamnionitis and sepsis are vital risk factors in BPD development.[15,16] Apoptosis is a common form of programmed cell death. A previous study showed that BCL2-binding component 3 (BBC3)-induced apoptosis is closely related to the mechanism of BPD.[17] Mitochondrial apoptosis is the most common deregulated form of apoptosis and has been demonstrated to play an essential role in cancer treatment.[18] However, to the best of our knowledge, there have been few reports on the effect of the mitochondrial and MEK1/2-ERK1/2 pathways in inflammation and apoptosis in BPD on VitD administration. We hypothesized that VitD treatment reduces inflammation and apoptosis through the mitochondria-mediated and MEK1/2-ERK1/2 signaling pathways involved in BPD. To test this hypothesis, we first studied the effects of VitD administration on lung structure, inflammation, and apoptosis in a BPD C57BL/6 mouse model. We found that VitD treatment restored alveolarization and reduced fibrosis and improved inflammation and apoptosis in mouse neonates with BPD. We then examined the effects of VitD pretreatment on mitochondrial apoptosis in BEAS-2B cells exposed to hyperoxia. We found that VitD pretreatment ameliorated mitochondria-mediated apoptosis. Finally, we detected diminished inflammation and apoptosis by chemically inhibiting or genetically silencing the Vitamin D receptor (VDR) in the MEK1/2-ERK1/2 signaling pathway of BEAS-2B cells. These results suggest that early intervention with VitD may provide a novel strategy for treating BPD in preterm infants.

Materials and Methods

Animals and Treatments

One-day-old C57BL/6 mice were purchased from JOINN Laboratories (Suzhou, China). The postnatal day 2 (PN2) newborn mice were randomly assigned to four groups: (1) RA control group, with intraperitoneal injections of saline in room air (RA), exposed to 21% O_2; (2) RA+VitD group, intraperitoneally injected with calcitriol in RA; (3) BPD mice were maintained under hyperoxia (85% O_2); and (4) BPD+VitD group, which was administered intraperitoneal injections of calcitriol under hyperoxia. The PN2 mouse neonates were exposed to 85% O_2 (hyperoxia, BPD) or 21% O_2 (normoxia, RA) until 14 days of age (PN14), as described previously.[19] All mice received an intraperitoneal injection of 5 μg/Kg calcitriol (AbMole, USA) or saline control from PN2 to PN14, daily, as described previously.[20] The PN14 mice were anesthetized for the removal of their lungs, which were frozen in liquid nitrogen for later use (Supplementary Figure 1A). The animal protocol was approved by the Ethics Committee of Soochow University (Protocol No. 2013LW003), and the experiments were performed in accordance with the NIH's Guide for the Care and Use of Laboratory Animals.

Lung Histology and Morphometry

The lungs were excised and fixed for 24 h in 10% formalin, embedded in paraffin, and stained with hematoxylin and eosin (HE). Lung morphometry, including mean linear intercept (MLI), radial alveolar count (RAC), and septal thickness were calculated as previously described.[21,22] MLI was calculated using Image J software by measuring the average distance between the intersects of alveolar septal tissue and a superimposed counting grid. RAC was calculated as the

number of septa intersected by each line drawn from the center of the respiratory bronchiole to the distal acinus. Alveolar septal wall thickness was estimated using ImageJ software. Masson's trichrome staining was used to assess peribronchial and alveolar fibrosis. Masson's trichrome staining was performed to evaluate collagen deposition in the alveoli by determining percent staining using Image J software.[9] The lung injury scoring parameters, including hyalinization, edema, alveolar wall thickening, and neutrophil infiltration, were scored in five randomly selected fields of each section. The severity of the pathological features was rated by a score of 0, 1, 2, 3, or 4, to indicate no/very mild, mild, moderate, severe, or very severe injury, respectively. The total score was the average score calculated within each group. A minimum of three sections per sample and a minimum of six fields per section were randomly chosen for evaluation in a blinded fashion. 10 mice per group were assessed with 3 technical replicates.

Reverse Transcription-Quantitative Polymerase Chain Reaction (RT-qPCR)

Total RNA was extracted using the TRIzol reagent (Invitrogen, USA). Complementary DNA (cDNA) was synthesized from the RNA with a reverse transcription kit (Takara, Japan), following the manufacturer's instructions, using a Veriti 96-Well Thermal Cycler (ThermoFisher, USA). The cDNA and primers were subjected to quantitative PCR (qPCR) using the SYBR Green Master Mix (Roche, Switzerland) and a LightCycler 480 ® II device. The primers used in this study are listed in Table 1. The glyceraldehyde-3-phosphate dehydrogenase (GAPDH) gene was used as a standardized internal control. The relative expression ratio was calculated using the $2^{-\Delta\Delta Ct}$ method.[23] 10 mice per group were assessed with 3 technical replicates.

Enzyme-Linked Immunosorbent Assay (ELISA)

Lung samples were frozen at −80°C until use. The frozen lung tissue was transferred to no-enzyme homogenization tubes and mechanically homogenized at −40°C for 10 min in a 4-fold volume of ice-cold 0.9% saline (1:4) in a grinding machine (Servicebio Biotech, Wuhan, China).

Then they were centrifuged at 200 × g (centrifuge model ST16R, Thermo Sorvall, USA). The protein concentration in each supernatant was then standardized for all samples. IL-6, IFN-γ, and TNF-α expression was examined using the mouse ELISA kit MU30038, according to the manufacturer's protocol (Bioswamp, Wuhan, China). 10 mice per group were assessed with 3 technical replicates.

Terminal Deoxynucleotidyl Transferase-Mediated dUTP Nick-End Labeling (TUNEL) Assay

Apoptosis levels were measured using the terminal deoxynucleotidyl transferase-mediated dUTP nick-end labeling (TUNEL) assay. Lungs from mice were immersed in 4% paraformaldehyde and embedded in paraffin. After deparaffinization, antigen retrieval, and blocking, the slides were stained with an in-situ cell death detection kit (Servicebio

Table 1 Sequences of Primers Used in the qRT-PCR

Gene	Species	Forward Sequence (5′-3′)	Reverse Sequence (5′-3′)
Il-6	Human	ACTCACCTCTTCAGAACGAATTG	CCATCTTTGGAAGGTTCAGGTTG
IFN-γ	Human	TCGGTAACTGACTTGAATGTCCA	TCGCTTCCCTGTTTTAGCTGC
TNF-α	Human	CCTCTCTCTAATCAGCCCTCTG	GAGGACCTGGGAGTAGATGAG
GAPDH	Human	GTCTCCTCTGACTTCAACAGCG	ACCACCCTGTTGCTGTAGCCAA
Il-6	Mouse	CAGGCGGTGCCTATGTCTC	CGATCACCCCGAAGTTCAGTAG
IFN-γ	Mouse	GCCACGGCACAGTCATTGA	TGCTGATGGCCTGATTGTCTT
TNF-α	Mouse	CTGAACTTCGGGGTGATCGG	GGCTTGTCACTCGAATTTTGAGA
GAPDH	Mouse	TGACCTCAACTACATGGTCTACA	CTTCCCATTCTCGGCCTTG

Abbreviations: BPD, Bronchopulmonary dysplasia; VitD, Vitamin D; RA, room air; VDR, Vitamin D Receptor; MAPK, mitogen-activated protein kinase; BBC3, BCL2-binding component 3; HE, hematoxylin and eosin; MLI, mean linear intercept; RAC, radial alveolar count; RT-qPCR, Reverse transcription-quantitative polymerase chain reaction; cDNA, Complementary DNA; qPCR, quantitative PCR; GAPDH, glyceraldehyde-3-phosphate dehydrogenase; ELISA, Enzyme-linked immunosorbent assay; TUNEL, Terminal deoxynucleotidyl transferase-mediated dUTP nick-end labeling; DMEM, Dulbecco's modified Eagle's medium; TEM, transmission electron microscopy; MMP, mitochondrial membrane potential; BSA, bovine serum albumin; PI, propidium iodide; MOI, multiplicity of infection; SD, standard deviation.

Biotech, Wuhan, China). DNA fragmentation-associated apoptosis was measured by visualizing the fluorescence images (Nikon DS-U3, Japan). Data were quantified by performing a manual cell count of TUNEL-positive cells for each section. The number of TUNEL-positive cells was counted in 10 fields per sample at 10X magnification by blinded investigators. 10 mice per group were assessed with 3 technical replicates.

Cell Culture and Treatment

The human lung epithelial cell line BEAS-2B was purchased from FuHeng BioLogy (FH0319, Shanghai, China) and cultured with 10% fetal bovine serum (FBS) and penicillin and streptomycin (100 mg/mL) in Dulbecco's modified Eagle's medium (DMEM) at 37 °C with 5% CO_2. The BEAS-2B cells were divided into five groups: (1) RA control group with no added agents in RA, (2) RA+VitD cells with added calcitriol maintained at RA; (3) BPD cells, maintained under hyperoxia; (4) BPD+VitD group with added calcitriol and maintained hyperoxia; and (5) BPD+VitD+inhibitor cells with added calcitriol and inhibitor, also maintained under hyperoxia. These cells were seeded in six-well plates, incubated for 24 h, and then cultured in DMEM containing 0.1% FBS for 6 h. Subsequently, the media were replaced with new media with or without the addition of 10 nM calcitriol (AbMole, USA)[24] or 1 mM VDR inhibitor TEI-9647 (GLPBIO, USA)[25] for 12 h. Then, these cells were cultured in the HeraCell 150i incubator (Thermo Fisher, USA) with an ambient oxygen concentration of RA (21% O_2, 5% CO_2) or hyperoxia (85% O_2, 5% CO_2) for 6 h[26,27] and harvested for subsequent experiments (Supplementary Figure 1B).

Transmission Electron Microscopy

The cells were collected and fixed in fresh transmission electron microscopy (TEM) fixative at 4 °C, overnight, followed by 1% osmium tetroxide treatment and dehydration. Later, cells were embedded in resin, sliced in ultrathin sections, and contrasted with uranyl acetate and lead citrate for electron microscopy. TEM images were obtained using the H7800 transmission electron microscope (Hitachi, Tokyo, Japan). We manually scored the abnormal mitochondrial structure, including structural rarefaction, and vacuole and cristae breaking in each group of cells. The severity of the abnormal mitochondrial structure was rated by a score of 0, 1, 2, and 3, to indicate no structural abnormality, mild, moderate, and severe structural abnormality, respectively.

Mitochondrial Membrane Potential Measurement

The mitochondrial membrane potential (MMP) was measured using the JC-1 Apoptosis Detection Kit (KGA601-KGA604, Keygen Biotech, Nanjing, China), according to the manufacturer's instructions. The treated cells were stained with JC-1 for 30 min at 37 °C. Next, the stained cells were collected and analyzed using a flow cytometer (Beckman Coulter Gallios, USA).

Western Blot Analysis

The mitochondrial pellet was extracted from the cell culture using the EXkine^{TM} Mitochondrion Extraction Kit (Abbkine USA) and resuspended in RIPA lysis buffer, which was frozen for Western blotting. Total protein using RIPA lysis buffer (Beyotime Institute of Biotechnology, China) containing 1% protease inhibitor. A 5 × loading buffer was added, and the mixture was boiled at 100 °C for 10 min. Proteins were transferred to polyvinylidene fluoride membranes (Millipore Corporation, USA). The membranes were blocked with 5% bovine serum albumin (BSA), followed by incubation with primary antibodies overnight at 4°C. The following primary antibodies were used: anti-phosphorylated (p)-MEK1/2 (1:10,000; Abcam, UK), anti-MEK1/2 (1:10,000; Abcam), anti-phosphorylated (p)-ERK1/2 (1:10,000; Abcam), anti-ERK1/2 (1:10,000; Abcam), anti-cleaved caspase-3 (1:1000; Cell Signaling, USA), anti-Bcl-2 (1:2000; Abcam), anti-Bax (1:2000; Abcam), and anti-GAPDH (1:5000; Abcam). Membranes were then incubated with HRP-conjugated secondary antibodies (1:5000; Abcam) for 1 h at room temperature. ECL reagent (Beyotime Institute of Biotechnology) was used for immunodetection and visualization using a Bio-Image Analysis System (Syngene, USA). Densitometric quantification was performed using ImageJ after normalization with GAPDH.

Apoptosis Assay by Flow Cytometry

Cell apoptosis was detected using the Annexin V-Alexa Fluor 647/PI apoptosis Assay Kit (FMSAV647-100; FcMACS, Nanjing, China). Cells were centrifuged at 200 × g and 800 rpm for 3 min, and the pellets were suspended and dyed with Annexin V-Alexa Fluor 647 and propidium iodide (PI) solution for 15 min at room temperature, without light. Stained cells were measured immediately using a flow cytometer (Beckman Coulter Gallios, USA).

Silencing VDR in BEAS-2B Cells

BEAS-2B cells were stably transfected with VDR-shRNA to silence the expression of VDR, according to the manufacturer's protocol (GeneChem, Shanghai, China). The cells were divided into five groups: (1) RA control group with no added agents; (2) RA+NC-shRNA cells transfected with NC-shRNA in RA; (3) BPD cells maintained under hyperoxia; (4) BPD+VitD cells with added calcitriol and maintained under hyperoxia; and (5) BPD+VitD+VDR-shRNA cells transfected with VDR-shRNA and added calcitriol, maintained under hyperoxia. In brief, BEAS-2B cells (1×10^5 per well) were seeded in six -well plates and cultured in DMEM for 24 h. Then, cells were infected with the shRNA lentiviral particles (GeneChem, Shanghai, China) at 100:1 multiplicity of infection (MOI), mixed gently, and incubated for 8 h. After 8 h of transduction, infected cells were replaced with DMEM and incubated for 48 h. Then, the infected cells were cultured in DMEM media with 0.5 μg/mL puromycin dihydrochloride (Sigma) for 48 h to select stably infected cells expressing the VDR-shRNA. The shRNA sequences were: VDR-shRNA 5′-cgAAGTGTTTGGCAATGAGAT-3`; and NC-shRNA 5′ -TTCTCCGAACGTGTCACGT-3`.

Statistical Analysis

Data were analyzed with GraphPad Prism 9.0 and represented by mean ± standard deviation (SD). Comparison among groups was performed using one-way ANOVA, followed by Tukey's multiple comparison test. Data normality was determined using the Shapiro–Wilk normality test. Inflammatory marker mRNA levels and Western blot were expressed relative to the average level of the control group. All data measurements and analysis were performed by investigators blinded to the experimental groups. The experiments were carried out three times independently and repeatedly. Statistical significance was set at $p < 0.05$.

Results

VitD Administration Mitigated Alveolar Simplification and Lung Fibrosis in Neonatal Mice with Hyperoxia-Induced Lung Injury

The lung volume was small, and the color was dim in the BPD lung as compared to the other groups. The volume and color of the lung in the BPD+VitD group were similar to those in the RA group. The lung injury score was used to evaluate the degree of lung injury. We found that the lung injury score was higher in BPD lung as compared to the other groups and VitD administration could decrease the score significantly. We evaluated the features of the BPD phenotype, such as alveolar lung simplification and abnormal fibrosis, in experimental BPD mice with HE and Masson's staining. Alveolarization was determined by calculating mean linear intercept (MLI), radial alveolar count (RAC), and septal thickness. Masson's trichrome staining was used to assess the peribronchial and alveolar fibrosis. As shown in Figure 1, hyperoxia led to aberrant lung morphometry, as evidenced by the increased alveolar size measured as MLI, decreased RAC, and enhanced septal thickness in the lungs. We found that treatment with VitD in newborn mice rescued impaired alveolarization and abnormal fibrosis in the lungs. We did not find any significant changes in the lung morphometric index of MLI, RAC, and septal thickness when we compared RA to RA+VitD groups. These results suggest that VitD may ameliorate hyperoxia-induced lung injury.

VitD Diminished Pro-Inflammatory Cytokines and Decreased Apoptosis in the Lungs of Mice Neonates with BPD

We examined the relative mRNA expression levels of the pro-inflammatory cytokines IL-6, IFN-γ, and TNF-α in the lungs of mice neonates with BPD. We found that newborn mice exposed to hyperoxia and treated with VitD showed significantly reduced pro-inflammatory cytokine expression levels compared to untreated mice (Figure 2A). This was further supported by the reduced levels of the pro-inflammatory cytokines IL-6, IFN-γ, and TNF-α detected in lung tissue

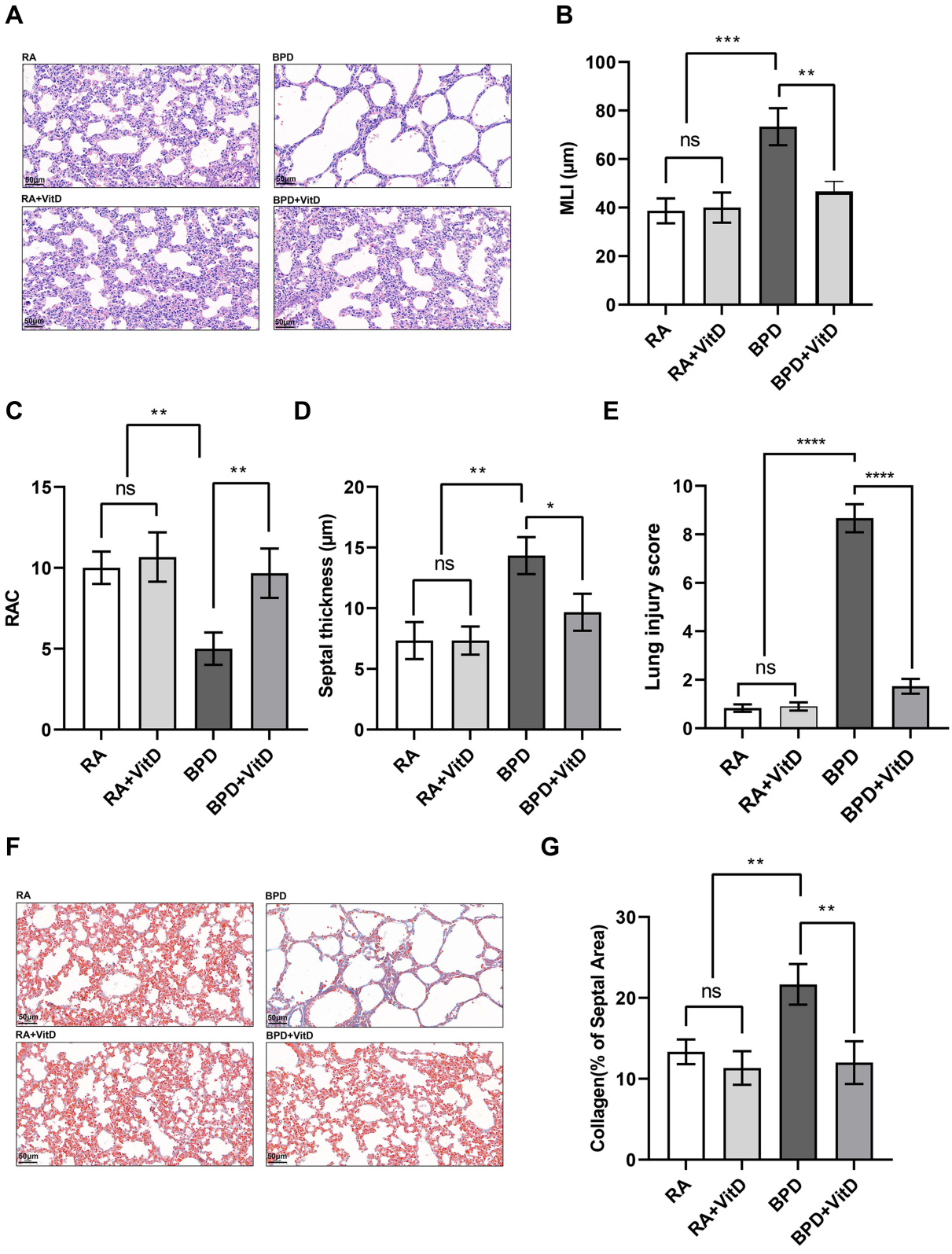

Figure 1 Vitamin D (VitD) decreases alveolar simplification and lung fibrosis induced by hyperoxia in newborn mice. (**A**–**E**) Hematoxylin and eosin images showing the characteristic simplification of lung alveolarization in the bronchopulmonary dysplasia group. VitD therapy improved lung alveolarization, as quantified by mean linear intercept, radial alveolar count, lung injury score, and septal thickness changes. (**F**–**G**) Representative Masson's trichrome staining of lung tissues. VitD treatment ameliorated lung fibrosis induced by hyperoxia, as quantified by changes in the collagen rate of the septal area. The results shown were observed in at least three independent experiments. N = 10 mice per group; scale bar = 50 μm; magnification at 20X. *p < 0.05; **p < 0.01; ****p < 0.0001.
Abbreviation: ns, not significant.

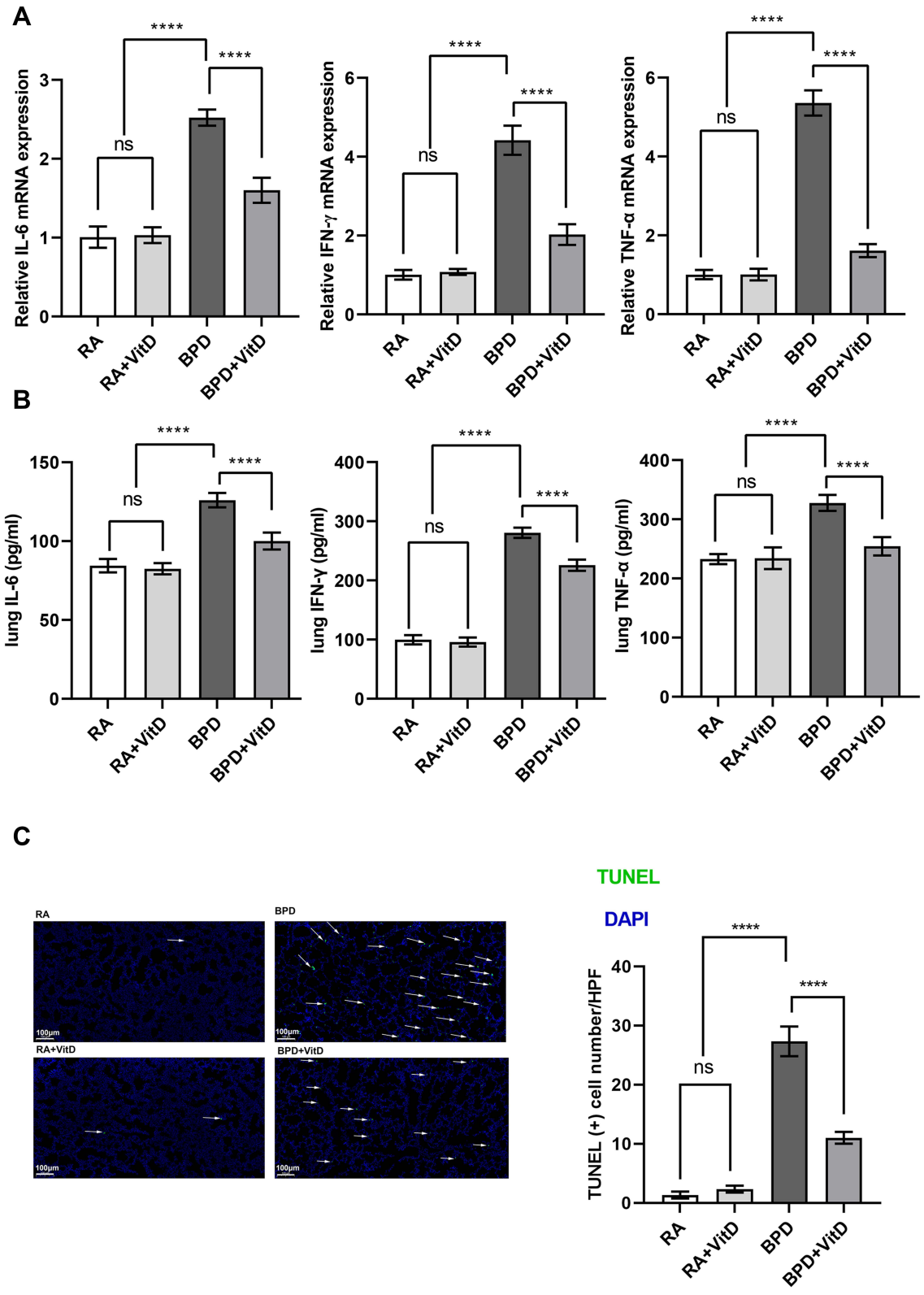

Figure 2 Vitamin D (VitD) treatment reduces the pro-inflammatory cytokines and represses the apoptosis in lungs of bronchopulmonary dysplasia (BPD) mice. (**A**) RT-qPCR detection of IL-6, IFN-γ, and TNF-α genes, showing their induction in the BPD mice and suppression by VitD treatment. (**B**) The protein levels of IL-6, IFN-γ, and TNF-α measured by ELISA showed their induction in the BPD mice and repression in the VitD treatment group. (**C**) The count of TUNEL-positive cells, detected by immunofluorescence, increased in the BPD mice and decreased with VitD treatment. TUNEL-positive cells were labeled with FITC fluorescence (green). The results shown were observed in at least three independent experiments. N = 10 mice per group; scale bar = 100 μm; magnification at × 10; ****p < 0.0001.

Abbreviations: DAPI, 4′6-diamidino-2-phenylindole; FITC, fluorescein isothiocyanate; ns, not significant.

by ELISA in the BPD+VitD group compared to the BPD control (Figure 2B). VitD treatment also reduced lung apoptosis in BPD+VitD neonate mice, as determined by TUNEL immunofluorescence (Figure 2C). We did not find any significant lung inflammation and apoptosis changes when comparing RA to RA+VitD groups. These findings indicate that VitD treatment attenuated hyperoxia-induced lung inflammation and apoptosis in experimental BPD mice.

Pretreatment with VitD Restored Apoptosis by Targeting the Mitochondrial Pathway in BEAS-2B Cells Exposed to Hyperoxia

The cellular mitochondrial apoptotic features were visualized by TEM. Abnormal mitochondria with vacuole formation and mitochondrial cristae breakage or disappearance were observed in BEAS-2B cells under hyperoxia. The abnormal mitochondria score was used to assess the degree of mitochondrial apoptosis. We found that the abnormal mitochondrial score was higher in BPD lung as compared to other groups and VitD administration could decrease the score significantly (Figure 3A). JC-1 staining of BEAS-2B cells assessed the loss of MMP using flow cytometry. We observed that hyperoxia significantly increased MMP loss when compared with normoxia. Furthermore, VitD pretreatment significantly reduced the loss of MMP in BEAS-2B cells exposed to hyperoxia (Figure 3B). Hyperoxia increased the relative protein expression of the mitochondrial apoptosis-related proteins cleaved caspase-3 and Bax, while Bcl-2 expression decreased in BEAS-2B cells under hyperoxia. VitD pretreatment significantly diminished cleaved caspase-3 and Bax expression and enhanced Bcl-2 expression (Figure 3C). We isolated mitochondria and demonstrated that the Bax/Bcl-2 ratio increased in the mitochondria in the BPD lung as compared to that in the other groups and VitD administration could decrease the ratio significantly (Figure 3D). We did not find any significant changes in these protein expression levels when we compared RA to RA+VitD. These results demonstrate that VitD mediates apoptosis by targeting the mitochondria-mediated pathway.

VitD Ameliorated Inflammation and Apoptosis by the Inhibition of VDR Through the MEK1/2-ERK1/2 Signaling Pathway in BEAS-2B Cells Under Hyperoxia

We investigated the mechanism by which VitD mediates inflammation and apoptosis in BEAS-2B cells under hyperoxia. We measured inflammation and apoptosis in response to hyperoxia in the presence or absence of the VDR inhibitor, TEI-9647. We found that the mRNA expression of IL-6, IFN-γ, and TNF-α was reduced by VitD administration after BPD and increased with the addition of the VDR inhibitor under hyperoxia (Figure 4A). We also found that the apoptotic rate detected by flow cytometry analysis was diminished in the BPD+VitD group and aggravated with the addition of VDR inhibitor under hyperoxia (Figure 4B and C). Western blotting showed that phosphorylation of MEK1/2 and ERK1/2 proteins was decreased in the BPD+VitD group. Interestingly, the VDR inhibitor activated the phosphorylation of these proteins in BEAS-2B cells pretreated with VitD under hyperoxia (Figure 4D–F). We did not find any significant changes in inflammation and apoptosis when comparing RA to RA+VitD. Collectively, these results suggest that VitD mitigates inflammation and apoptosis by targeting the MEK1/2-ERK1/2 pathway.

Silencing VDR Showed That VitD Attenuated Inflammation and Apoptosis via the MEK1/2-ERK1/2 Pathway in BEAS-2B Cells Exposed to Hyperoxia

To continue investigating the potential role of VitD in inflammation and apoptosis, VDR-shRNA was used to silence VDR in BEAS-2B cells that were exposed to hyperoxia. We found decreased mRNA expression of IL-6, IFN-γ, and TNF-α in BEAS-2B cells pretreated with VitD under hyperoxia. In contrast, VDR-shRNA expression in BEAS-2B cells resulted in a significant increase in IL-6, IFN-γ, and TNF-α expression (Figure 5A). Flow cytometry analysis detected a reduced apoptotic rate after pretreatment with VitD under hyperoxia, while the shRNA-mediated VDR silencing increased apoptosis in BEAS-2B cells (Figure 5B and C). Knockdown of the VDR gene also resulted in increased phosphorylation of MEK1/2 and ERK1/2 proteins, as shown by the Western blot of BEAS-2B cells exposed to hyperoxia (Figure 5D–F). We did not find any significant changes in inflammation and apoptosis when we compared RA with RA +NC-shRNA. These results indicate that VitD exerts protective effects and attenuates inflammation and apoptosis via the MEK1/2-ERK1/2 signaling pathway in response to hyperoxia.

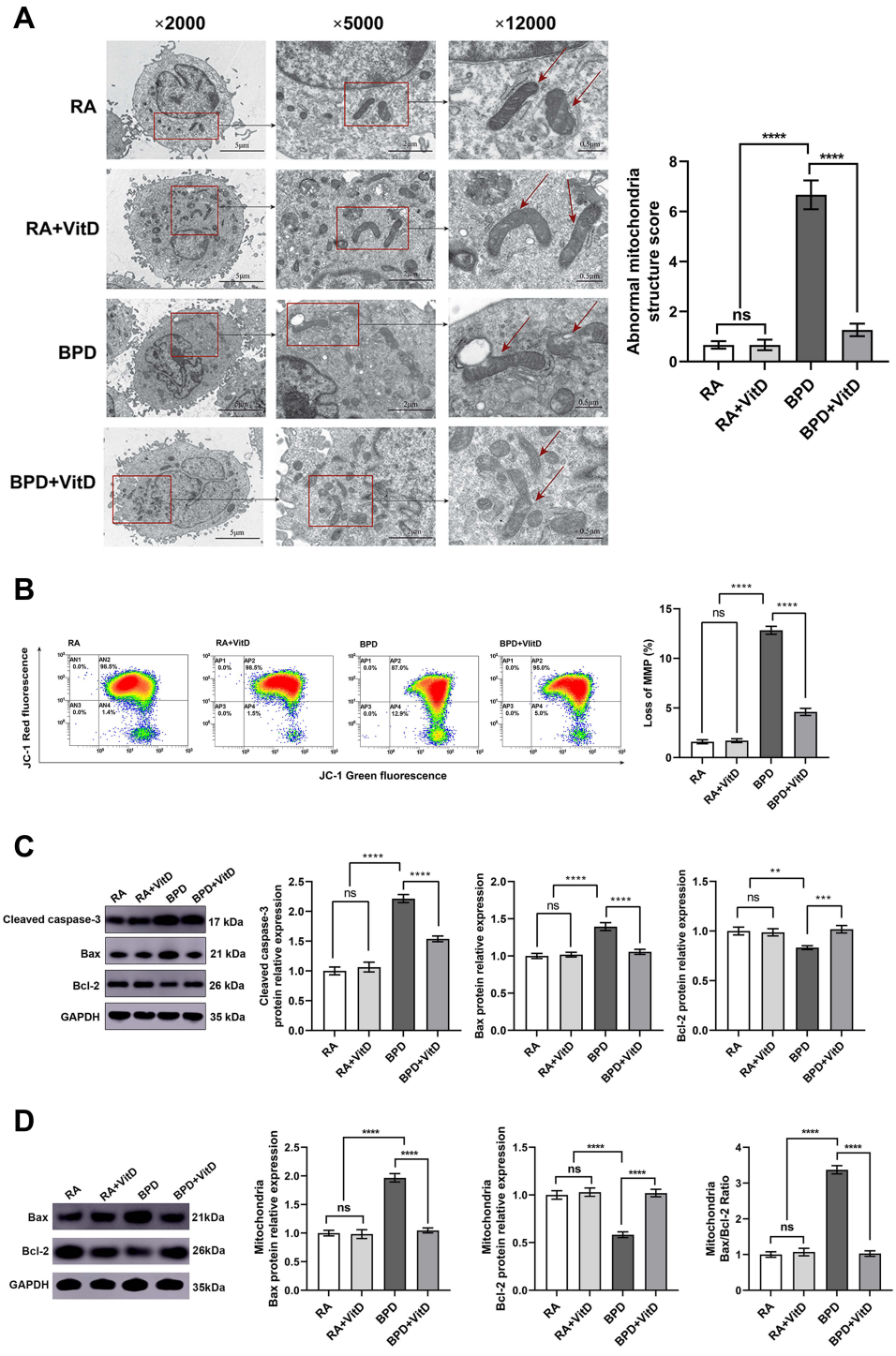

Figure 3 Vitamin D (VitD) ameliorates apoptosis by targeting its mitochondrial pathway in BEAS-2B cells under hyperoxia. (**A**) Ultrastructural changes were observed under TEM (magnification at × 2000, × 5000, × 12,000). The mitochondrial morphological characteristics (red arrows) are shown, as quantified by the abnormal mitochondrial structure score. Abnormal mitochondria were detected in the bronchopulmonary dysplasia (BPD)group, while the BPD+VitD group showed normal mitochondrial morphology. (**B**) Mitochondrial membrane potential (MMP) was determined by flow cytometry using JC-1 staining. The upper right quadrant (AP2) is labeled as JC-1 red (intact fraction, high MMP) and the lower right quadrant (AP4) as JC-1 green (damaged fraction, low MMP). The bar graph shows the quantitative analysis of the loss of MMP. VitD pretreatment reversed the loss of MMP in BEAS-2B cells induced by hyperoxia. Fifty thousand cells were analyzed in each sample. (**C**) The repression of cleaved caspase-3 and Bax detected by Western blot in the VitD treatment group compared to the BPD group. The Bcl-2 expression increased with VitD pretreatment in relation to the BPD group. (**D**) Bax expression increased and Bcl-2 decreased in mitochondria detected by Western blot in the BPD group. The Bax/Bcl-2 ratio decreased with VitD pretreatment in relation to the BPD group. Western blot densitometric values were normalized to GAPDH. The results shown were observed in at least three independent experiments. N (Number of samples per group) = 10. ** $p < 0.01$, *** $p < 0.001$, **** $p < 0.0001$.

Abbreviation: ns, not significant.

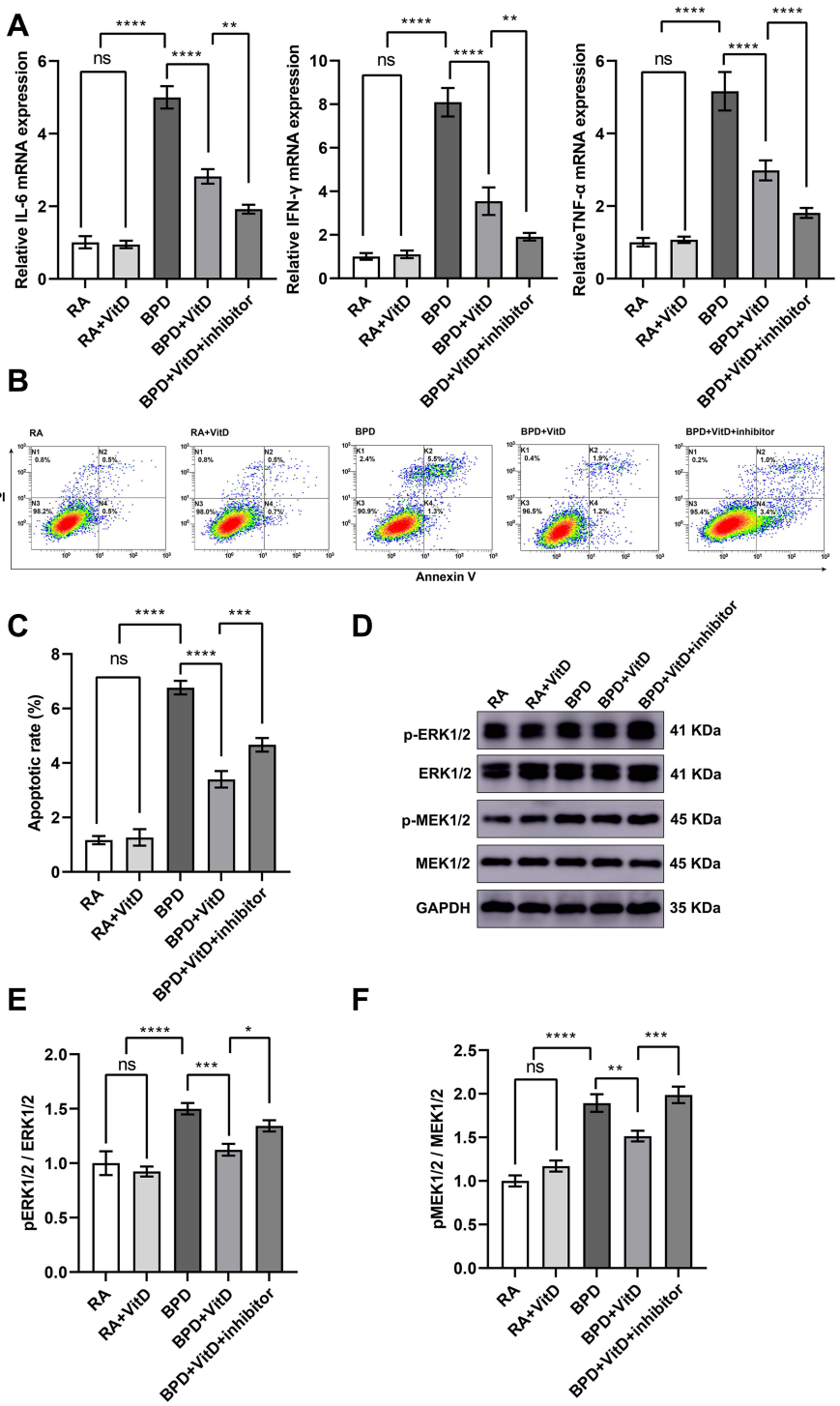

Figure 4 Inhibition of VDR regulates inflammation and apoptosis through the MEK1/2-ERK1/2 pathway in BEAS-2B cells exposed to hyperoxia. (**A**) The RT-qPCR detected repression of IL-6, IFN-γ, and TNF-α mRNA levels in the BPD+VitD group in relation to the BPD group, which were further repressed with the addition of the VDR inhibitor TEI-9647. (**B** and **C**) Proportions of living and apoptotic cells were detected by flow cytometry analysis. The percentage of surviving cells is shown in the lower left quadrant (K3), early apoptotic cells are shown in the lower right quadrant (K4), and late apoptotic cells are shown in the upper right quadrant (K2). The apoptotic cell rate (K2+K4) decreased in the BPD+VitD group and increased with the addition of the inhibitor TEI-9647. Ten thousand cells were analyzed in each sample. (**D**–**F**) Western blot detected MEK1/2 and ERK1/2 phosphorylation inhibition in the BPD+VitD group, which were reversed by TEI-9647 treatment. Graphs show the quantitative analysis of the protein expression levels in the five groups. Western blot densitometric values were normalized to GAPDH. Results shown were observed in at least three independent experiments. N (Number of samples per group) = 10. *p < 0.05; **p < 0.01, ***p < 0.001, ****p < 0.0001.

Abbreviation: ns, not significant.

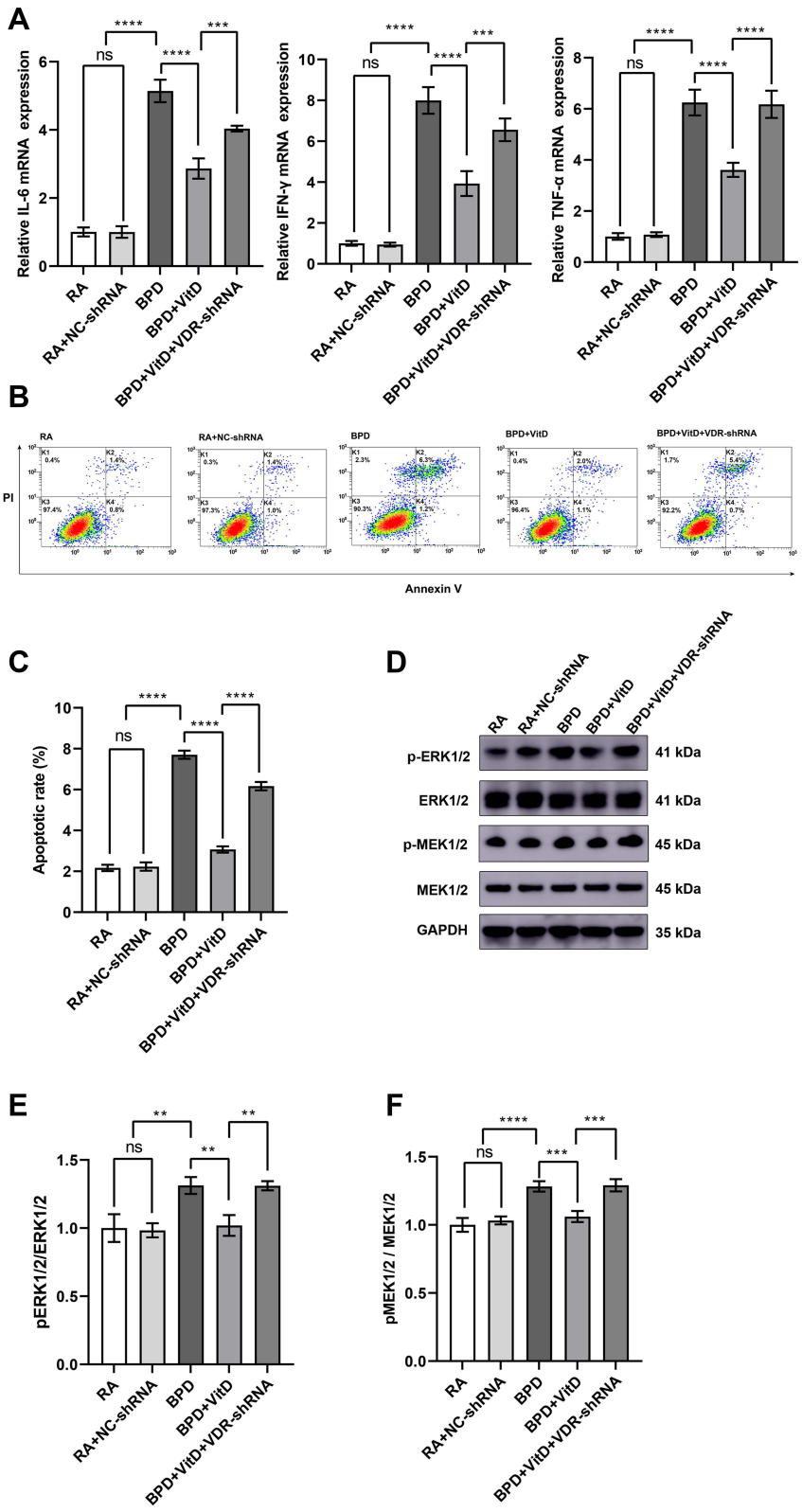

Figure 5 VDR Silencing mediates inflammation and apoptosis via the MEK1/2-ERK1/2 pathway in BEAS-2B cells under hyperoxia. (**A**) IL-6, IFN-γ, and TNF-α transcription were repressed in the BPD+VitD group, while VDR silencing in the BPD+VitD+VDR-shRNA restores the mRNA levels of these genes. (**B** and **C**) Lower percentages of early and late apoptotic cells (K2+K4) detected by flow cytometry were reduced in the BPD+VitD group and increased by the performance of VDR-shRNA. Ten thousand cells were analyzed in each sample. (**D**–**F**) Phosphorylation of MEK1/2 and ERK1/2 were reduced in the BPD+VitD group and reversed by the expression of VDR-shRNA. Western blot densitometric values were normalized to GAPDH. The results shown were observed in at least three independent experiments. N (Number of samples per group) = 10. **p < 0.01, ***p < 0.001, ****p < 0.0001. **Abbreviation**: ns, not significant.

Discussion

In the current study, we demonstrated that VitD treatment improves arrested lung development and decreases inflammation and apoptosis in the lungs of neonatal mice with BPD. We also showed that VitD pretreatment ameliorated apoptosis and inflammation by targeting the mitochondrial apoptosis pathway and the MEK1/2-ERK1/2 signaling pathway in BEAS-2B cells under hyperoxia.

BPD often results from complex mechanisms that lead to compromised alveolarization and aberrant repair of injury in the developing lung under hyperoxia, infection, and mechanical ventilation.[28] In this study, we used a mouse model exposed to 85% O2 from PN2 to PN14 to mimic BPD in vivo. Subsequently, we analyzed the lung tissues by HE staining to confirm BPD establishment at PN14. The pathological changes in BPD lungs revealed by HE staining included alveolar simplification and reduction of RAC, as well as impaired alveolarization. We also observed the histopathology of BPD lung cells with Masson´s trichrome staining and TUNEL assay to assess fibrosis and apoptosis in the lungs. These results showed increased fibrosis and apoptosis in the lungs of mice with BPD. These findings are consistent with those of previous studies.[29–31]

Although our understanding of BPD has increased, the involvement of VitD in the mechanisms of BPD remains unclear. Several hypotheses have been proposed to explain the underlying mechanisms involved in activating inflammation and apoptosis promoted by hyperoxia. The release of various pro-inflammatory cytokines is among the ways in which hyperoxia induces lung injury.[32,33] The pathological mechanisms of inflammation-mediated pathways such as MAPK/NF-κB and A2aR signaling are also dysregulated in BPD.[34] Furthermore, preterm infants with BPD have elevated protein levels of pro-inflammatory cytokines and an increased number of inflammatory cells in their tracheal aspirates.[35] Several crucial molecules have been identified in the process of inflammatory cell recruitment, including cytokines such as IL-6, IFN-γ, and TNF-α, which were shown to be increased in BPD.[36,37] Hyperoxia is one of the most potent risk factors for inflammation in preterm infants.[38] This may be due to the different airway and lung tissue microenvironments between RA and hyperoxia. We inferred that the increase in IL-6, IFN-γ, and TNF-α expression under hyperoxic conditions was not only due to the increment in inflammatory cells but also due to the activation of the upstream signaling pathways, which regulate IL-6, IFN-γ, and TNF-α expression. This phenomenon observed in our study is consistent with that observed in previous studies.

Calcitriol, the active form of VitD, is involved in cell proliferation and inflammation. VitD deficiency may contribute to cellular inflammatory responses.[39] Low levels of VitD observed in the plasma of newborn mice caused the deterioration of allergic airway inflammation, suggesting that VitD deficiency affected inflammation.[40] It has been demonstrated that VitD deficiency contributes to lung fibrosis, and VitD supplementation combined with anti-fibrotic therapeutics can ameliorate this symptom.[41,42] Previous research has frequently shown the anti-inflammatory effects of VitD in some human diseases, implicating VitD as a possible anti-inflammation therapy.[43,44] In addition, some researchers have demonstrated that VitD treatment can protect against BPD, and VitD supplementation can ameliorate alveolar development in a BPD animal model by reducing the release of inflammatory factors.[45,46] In our study, the expression of IL-6, IFN-γ, and TNF-α increased in BPD induced by hyperoxia, which was significantly decreased with application of calcitriol in the mice. We also found that VitD can reduce lung collagen content, ameliorate alveolar simplification, and blunt lung fibrosis in a BPD animal model. Altogether, hyperoxia-induced lung injury in BPD can be relieved by administering VitD in mice.

We further measured the protective effects of VitD in vitro using human BEAS-2B cells exposed to hyperoxia for 6 h.[27] We detected morphological alterations in mitochondria using TEM, MMP with flow cytometry, and apoptosis by Western blotting. Abnormal mitochondria with vacuole formation and mitochondrial cristae breakage or disappearance were observed in BEAS-2B cells under hyperoxia. We found that the mitochondrial structure was damaged in the BPD group and was restored with VitD administration. Another finding was that VitD treatment reversed the changes observed in cleaved caspase-3, Bax, and Bcl-2 expression after hyperoxia treatment. We also found that the Bax/Bcl-2 ratio was decreased in isolated-mitochondria with VitD pretreatment. These proteins are associated with mitochondrial apoptosis.[47–49] Mitochondrial apoptosis is considered a strong apoptotic reaction that initiates in the mitochondria, and leads to decreased anti-apoptosis protein biosynthesis. A critical molecular function mediating apoptosis is opening the mitochondrial permeability transition in response to the initiation of mitochondrial apoptosis. Many pathways mediate mitochondrial membrane permeabilization, and the most

important are the mitochondrial and MAPK signaling pathways,[50] in which the MMP loss is increased, and abnormal mitochondria are observed.[51,52] Our study found that hyperoxia induced the loss of MMP, and the apoptotic rate decreased with VitD pretreatment. In conclusion, we showed that hyperoxia resulted in persistent mitochondrial apoptosis and that VitD pretreatment can inhibit this effect in BEAS-2B cells under hyperoxia. The above evidence indicates that VitD inhibits apoptosis by targeting the mitochondrion-mediated pathway, which supports the mechanistic role of mitochondrial apoptosis in the development of BPD (Figure 6).

The MEK1/2-ERK1/2 pathway is central to many cellular processes[53] and is typically stimulated in some inflammatory diseases and is related to apoptosis. This pathway also plays a crucial role in some respiratory diseases, such as acute lung injury and lung cancer, and is known to regulate lung inflammatory responses and acute lung injuries.[13,14] To investigate whether this molecular mechanism is involved in BPD with VitD application, we used TEI-9647, an inhibitor of VDR, to measure inflammation and apoptosis levels. It has been reported that VitD exerts its biological effects by binding to VDR and regulating multiple signal pathways.[54] In our in vitro assay, we noted that increased apoptosis and inflammation were related to increased phosphorylation of MEK1/2 and ERK1/2 proteins in the BPD group, suggesting the involvement of the MEK1/2-ERK1/2 pathway in the process of inflammation and apoptosis. We also detected decreased phosphorylation of MEK1/2 and ERK1/2, reduced levels of IL-6, IFN-γ, and TNF-α, and the repressed apoptotic rate was reversed by the addition of the VDR inhibitor TEI-9647. These results suggested that VitD relieved inflammation and apoptosis via the MEK1/2–ERK1/2 pathway. We also knocked down the VDR gene by expressing the VDR-shRNA construct, and we observed that NC-shRNA had no effect on cells. In this experiment, we noted that the effects of VitD on inflammation and apoptosis were reversed by VDR-shRNA mediated signaling in BEAS-2B cells exposed to hyperoxia. Thus, the improvement of inflammation and apoptosis with VitD pretreatment was related to the MEK1/2-ERK1/2 pathway. These results strongly indicated that VitD exerted a protective regulatory function via the MEK1/2-ERK1/2 pathway during BPD (Figure 6).

Given the above results, we propose that VitD exerts a protective effect on diseased lung structures and ameliorates apoptosis and inflammation by targeting the mitochondrial apoptosis pathway and the MEK1/2-ERK1/2 signaling pathway in BPD pathogenesis. Few relevant studies have been reported previously. Therefore, our study addresses previous gaps in knowledge regarding the molecular mechanisms implicated in BPD. There were a few limitations to this study. We were unable to evaluate the molecular mechanism in the mouse model and used only one VDR inhibitor and

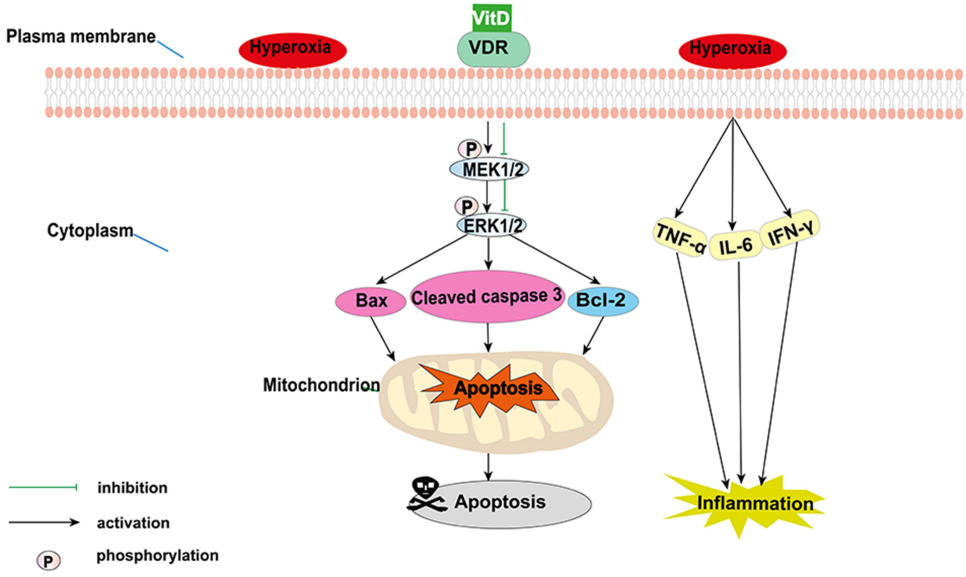

Figure 6 Vitamin D (VitD) modulates the mitochondrial apoptosis pathway and the MEK1/2-ERK1/2 pathway in bronchopulmonary dysplasia. Hyperoxia induces MEK1/2 and ERK1/2 phosphorylation and releases pro-inflammatory cytokines. Subsequently, the expression of mitochondrial apoptosis-related proteins (cleaved caspase-3, Bax, and Bcl-2) are altered. VitD pretreatment reversed these hyperoxia-induced alterations, inhibiting inflammation and apoptosis.

one cell line in the present study. Moreover, we could not specifically analyze mitochondrial apoptosis in the MEK1/2 and ERK1/2 signaling pathways. Therefore, further studies need to be performed to confirm the findings reported here.

Conclusion

In summary, We found that VitD treatment ameliorated apoptosis and inflammation by targeting the mitochondrial pathway and via the MEK1/2-ERK1/2 signaling pathway in BPD. We intend to observe the molecular mechanism in animal models with inhibitors and study the relationship between mitochondrial apoptosis and the MEK1/2 and ERK1/2 signaling pathways. Nevertheless, this study provides potential therapeutic options and targets for BPD in preterm infants.

Author Contributions

All authors made a significant contribution to the work reported, whether that is in the conception, study design, execution, acquisition of data, analysis and interpretation, or in all these areas; took part in drafting, revising or critically reviewing the article; gave final approval of the version to be published; have agreed on the journal to which the article has been submitted; and agree to be accountable for all aspects of the work. The overall figures remained the property/ copyright of all authors.

Funding

This study was financially supported by the National Natural Science Foundation (NNSF) of China (No. 81971423, 81771626), Jiangsu Key Talent Program of Maternal and Child Health (No. FRC201731), Medical Research Project of Jiangsu Health and Family Planning Commission of China (No. ZD2021013) and Jiangsu Provincial Key Social Development Project of China (No. BE2020658).

Disclosure

The authors report no conflicts of interest in this work.

References

1. Thébaud B, Goss KN, Laughon M, et al. Bronchopulmonary dysplasia. *Nat Rev Dis Primers*. 2019;5(1):78. doi:10.1038/s41572-019-0127-7
2. Liu ZQ, Li XX, Qiu SQ, et al.Vitamin D contributes to mast cell stabilization. *Allergy*. 2017;72(8):1184–1192.
3. Corachán A, Ferrero H, Aguilar A, et al. Inhibition of tumor cell proliferation in human uterine leiomyomas by vitamin D via Wnt/β-catenin pathway. *Fertil Steril*. 2019;111(2):397–407. doi:10.1016/j.fertnstert.2018.10.008
4. Schardey J, Globig A-M, Janssen C, et al. Vitamin D inhibits pro-inflammatory T cell function in patients with inflammatory bowel disease. *J Crohns Colitis*. 2019;13(12):1546–1557. doi:10.1093/ecco-jcc/jjz090
5. Tzilas V, Bouros E, Barbayianni I, et al. Vitamin D prevents experimental lung fibrosis and predicts survival in patients with idiopathic pulmonary fibrosis. *Pulm Pharmacol Ther*. 2019;55:17–24. doi:10.1016/j.pupt.2019.01.003
6. Mao X, Qiu J, Zhao L, et al. Vitamin D and IL-10 deficiency in preterm neonates with bronchopulmonary dysplasia. *Front Pediatr*. 2018;6:246. doi:10.3389/fped.2018.00246
7. Chen C, Weng H, Zhang X, et al. Low-dose vitamin D protects hyperoxia-induced bronchopulmonary dysplasia by inhibiting neutrophil extracellular traps. *Front Pediatr*. 2020;8:335. doi:10.3389/fped.2020.00335
8. Zhen H, Hu H, Rong G, Huang X, Tan C, Yu X. VitA or VitD ameliorates bronchopulmonary dysplasia by regulating the balance between M1 and M2 macrophages. *Biomed Pharmacother*. 2021;141:111836. doi:10.1016/j.biopha.2021.111836
9. Kose M, Bastug O, Sonmez MF, et al. Protective effect of vitamin D against hyperoxia-induced lung injury in newborn rats. *Pediatr Pulmonol*. 2017;52(1):69–76. doi:10.1002/ppul.23500
10. Yao L, Shi Y, Zhao X, et al. Vitamin D attenuates hyperoxia-induced lung injury through downregulation of Toll-like receptor 4. *Int J Mol Med*. 2017;39(6):1403–1408. doi:10.3892/ijmm.2017.2961
11. Song J, Liu W, Wang J, et al. GALNT6 promotes invasion and metastasis of human lung adenocarcinoma cells through O-glycosylating chaperone protein GRP78. *Cell Death Dis*. 2020;11(5):352. doi:10.1038/s41419-020-2537-6
12. Stivala S, Codilupi T, Brkic S, et al. Targeting compensatory MEK/ERK activation increases JAK inhibitor efficacy in myeloproliferative neoplasms. *J Clin Invest*. 2019;129(4):1596–1611. doi:10.1172/JCI98785
13. Yamakawa K, Yokohira M, Nakano Y, Kishi S, Kanie S, Imaida K. Activation of MEK1/2-ERK1/2 signaling during NNK-induced lung carcinogenesis in female A/J mice. *Cancer Med*. 2016;5(5):903–913. doi:10.1002/cam4.652
14. Long ME, Gong K-Q, Eddy WE, et al. MEK1 regulates pulmonary macrophage inflammatory responses and resolution of acute lung injury. *JCI Insight*. 2019;4(23). doi:10.1172/jci.insight.132377
15. Villamor-Martinez E, Álvarez-Fuente M, Ghazi AMT, et al. Association of chorioamnionitis with bronchopulmonary dysplasia among preterm infants: a systematic review, meta-analysis, and metaregression. *JAMA Netw Open*. 2019;2(11):e1914611. doi:10.1001/jamanetworkopen.2019.14611

16. Poets CF, Lorenz L. Prevention of bronchopulmonary dysplasia in extremely low gestational age neonates: current evidence. *Arch Dis Child Fetal Neonatal Ed*. 2018;103(3):F285–F291. doi:10.1136/archdischild-2017-314264
17. Shrestha AK, Gopal VYN, Menon RT, Hagan JL, Huang S, Shivanna B. Lung omics signatures in a bronchopulmonary dysplasia and pulmonary hypertension-like murine model. *Am J Physiol Lung Cell Mol Physiol*. 2018;315(5):L734–L741. doi:10.1152/ajplung.00183.2018
18. Lopez J, Tait SWG. Mitochondrial apoptosis: killing cancer using the enemy within. *Br J Cancer*. 2015;112(6):957–962. doi:10.1038/bjc.2015.85
19. Sucre JMS, Vickers KC, Benjamin JT, et al. Hyperoxia injury in the developing lung is mediated by mesenchymal expression of Wnt5A. *Am J Respir Crit Care Med*. 2020;201(10):1249–1262. doi:10.1164/rccm.201908-1513OC
20. de Oliveira LRC, Mimura LAN, Fraga-Silva TF, et al. Calcitriol prevents neuroinflammation and reduces blood-brain barrier disruption and local macrophage/microglia activation. *Front Pharmacol*. 2020;11:161. doi:10.3389/fphar.2020.00161
21. Das P, Acharya S, Prahaladan VM, et al. Chitin-derived AVR-48 prevents experimental bronchopulmonary dysplasia (BPD) and BPD-associated pulmonary hypertension in newborn mice. *Int J Mol Sci*. 2021;22(16):8547. doi:10.3390/ijms22168547
22. Gouveia L, Kraut S, Hadzic S, et al. Lung developmental arrest caused by PDGF-A deletion: consequences for the adult mouse lung. *Am J Physiol Lung Cell Mol Physiol*. 2020;318(4):L831–L843. doi:10.1152/ajplung.00295.2019
23. Schmittgen TD, Livak KJ. Analyzing real-time PCR data by the comparative C(T) method. *Nat Protoc*. 2008;3(6):1101–1108. doi:10.1038/nprot.2008.73
24. Bi C-S, Li X, Qu H-L, et al. Calcitriol inhibits osteoclastogenesis in an inflammatory environment by changing the proportion and function of T helper cell subsets (Th2/Th17). *Cell Prolif*. 2020;53(6):e12827. doi:10.1111/cpr.12827
25. Radujkovic A, Schnitzler P, Ho AD, Dreger P, Luft T. Low serum vitamin D levels are associated with shorter survival after first-line azacitidine treatment in patients with myelodysplastic syndrome and secondary oligoblastic acute myeloid leukemia. *Clin Nutr*. 2017;36(2):542–551. doi:10.1016/j.clnu.2016.01.021
26. Chen X-Q, Wu S-H, Luo -Y-Y, et al. Lipoxin A attenuates bronchopulmonary dysplasia via upregulation of Let-7c and downregulation of TGF-β signaling pathway. *Inflammation*. 2017;40(6):2094–2108. doi:10.1007/s10753-017-0649-7
27. Zhang L, Bai X, Yan W. LncRNA-MALAT1, as a biomarker of neonatal BPD, exacerbates the pathogenesis of BPD by targeting miR-206. *Am J Transl Res*. 2021;13(2):462–479.
28. Kalikkot Thekkeveedu R, Guaman MC, Shivanna B. Bronchopulmonary dysplasia: a review of pathogenesis and pathophysiology. *Respir Med*. 2017;132:170–177. doi:10.1016/j.rmed.2017.10.014
29. Chaubey S, Thueson S, Ponnalagu D, et al. Early gestational mesenchymal stem cell secretome attenuates experimental bronchopulmonary dysplasia in part via exosome-associated factor TSG-6. *Stem Cell Res Ther*. 2018;9(1):173. doi:10.1186/s13287-018-0903-4
30. Moreira A, Winter C, Joy J, et al. Intranasal delivery of human umbilical cord Wharton's jelly mesenchymal stromal cells restores lung alveolarization and vascularization in experimental bronchopulmonary dysplasia. *Stem Cells Transl Med*. 2020;9(2):221–234. doi:10.1002/sctm.18-0273
31. Willis GR, Fernandez-Gonzalez A, Anastas J, et al. Mesenchymal stromal cell exosomes ameliorate experimental bronchopulmonary dysplasia and restore lung function through macrophage immunomodulation. *Am J Respir Crit Care Med*. 2018;197(1):104–116. doi:10.1164/rccm.201705-0925OC
32. Ashley SL, Sjoding MW, Popova AP, et al. Lung and gut microbiota are altered by hyperoxia and contribute to oxygen-induced lung injury in mice. *Sci Transl Med*. 2020;12(556). doi:10.1126/scitranslmed.aau9959
33. Hirsch K, Taglauer E, Seedorf G, et al. Perinatal hypoxia-inducible factor stabilization preserves lung alveolar and vascular growth in experimental bronchopulmonary dysplasia. *Am J Respir Crit Care Med*. 2020;202(8):1146–1158. doi:10.1164/rccm.202003-0601OC
34. Zhao W, Ma L, Cai C, Gong X. Caffeine inhibits NLRP3 inflammasome activation by suppressing MAPK/NF-κB and A2aR signaling in LPS-induced THP-1 macrophages. *Int J Biol Sci*. 2019;15(8):1571–1581. doi:10.7150/ijbs.34211
35. Savani RC. Modulators of inflammation in bronchopulmonary dysplasia. *Semin Perinatol*. 2018;42(7):459–470. doi:10.1053/j.semperi.2018.09.009
36. Witkowski SM, de Castro EM, Nagashima S, et al. Analysis of interleukins 6, 8, 10 and 17 in the lungs of premature neonates with bronchopulmonary dysplasia. *Cytokine*. 2020;131:155118. doi:10.1016/j.cyto.2020.155118
37. Cui TX, Fulton CT, Brady AE, Zhang Y-J, Goldsmith AM, Popova AP. Lung CD103dendritic cells and Clec9a signaling are required for neonatal hyperoxia-induced inflammatory responses to rhinovirus infection. *Am J Physiol Lung Cell Mol Physiol*. 2021;320(2):L193–L204. doi:10.1152/ajplung.00334.2019
38. Huang D, Fang F, Xu F. Hyperoxia induces inflammation and regulates cytokine production in alveolar epithelium through TLR2/4-NF-κB-dependent mechanism. *Eur Rev Med Pharmacol Sci*. 2016;20(7):1399–1410.
39. Ferder M, Inserra F, Manucha W, Ferder L. The world pandemic of vitamin D deficiency could possibly be explained by cellular inflammatory response activity induced by the renin-angiotensin system. *Am J Physiol Cell Physiol*. 2013;304(11):C1027–C1039. doi:10.1152/ajpcell.00403.2011
40. Huang F, Ju Y-H, Wang H-B, Li Y-N. Maternal vitamin D deficiency impairs Treg and Breg responses in offspring mice and deteriorates allergic airway inflammation. *Allergy Asthma Clin Immunol*. 2020;16:89. doi:10.1186/s13223-020-00487-1
41. Han H, Chung SI, Park HJ, et al. Obesity-induced vitamin D deficiency contributes to lung fibrosis and airway hyperresponsiveness. *Am J Respir Cell Mol Biol*. 2021;64(3):357–367. doi:10.1165/rcmb.2020-0086OC
42. Sari E, Oztay F, Tasci AE. Vitamin D modulates E-cadherin turnover by regulating TGF-β and Wnt signalings during EMT-mediated myofibroblast differentiation in A459 cells. *J Steroid Biochem Mol Biol*. 2020;202:105723. doi:10.1016/j.jsbmb.2020.105723
43. Fitch N, Becker AB, HayGlass KT. Vitamin D [1,25(OH)2D3] differentially regulates human innate cytokine responses to bacterial versus viral pattern recognition receptor stimuli. *J Immunol*. 2016;196(7):2965–2972. doi:10.4049/jimmunol.1500460
44. Anderson J, Do LAH, Toh ZQ, et al. Vitamin D induces differential effects on inflammatory responses during bacterial and/or viral stimulation of human peripheral blood mononuclear cells. *Front Immunol*. 2020;11:602. doi:10.3389/fimmu.2020.00602
45. Liu C, Chen Z, Li W, Huang L, Zhang Y. Vitamin D enhances alveolar development in antenatal lipopolysaccharide-treated rats through the suppression of interferon-γ production. *Front Immunol*. 2017;8:1923. doi:10.3389/fimmu.2017.01923
46. Mandell E, Seedorf G, Gien J, Abman SH. Vitamin D treatment improves survival and infant lung structure after intra-amniotic endotoxin exposure in rats: potential role for the prevention of bronchopulmonary dysplasia. *Am J Physiol Lung Cell Mol Physiol*. 2014;306(5):L420–L428. doi:10.1152/ajplung.00344.2013
47. Hauseman ZJ, Harvey EP, Newman CE, et al. Homogeneous oligomers of pro-apoptotic BAX reveal structural determinants of mitochondrial membrane permeabilization. *Mol Cell*. 2020;79(1):68–83.e7. doi:10.1016/j.molcel.2020.05.029

48. Tan Z, Xiao L, Tang M, et al. Targeting CPT1A-mediated fatty acid oxidation sensitizes nasopharyngeal carcinoma to radiation therapy. *Theranostics*. 2018;8(9):2329–2347. doi:10.7150/thno.21451
49. Ngoi NYL, Choong C, Lee J, et al. Targeting mitochondrial apoptosis to overcome treatment resistance in cancer. *Cancers*. 2020;12(3):574. doi:10.3390/cancers12030574
50. Sorrentino G, Comel A, Mantovani F, Del Sal G. Regulation of mitochondrial apoptosis by Pin1 in cancer and neurodegeneration. *Mitochondrion*. 2014;19(Pt A):88–96. doi:10.1016/j.mito.2014.08.003
51. Yang Y, Wang G, Wu W, et al. Camalexin induces apoptosis via the ROS-ER stress-mitochondrial apoptosis pathway in AML cells. *Oxid Med Cell Longev*. 2018;2018:7426950. doi:10.1155/2018/7426950
52. Pan X, Yan D, Wang D, et al. Mitochondrion-mediated apoptosis induced by acrylamide is regulated by a balance between Nrf2 antioxidant and MAPK signaling pathways in PC12 cells. *Mol Neurobiol*. 2017;54(6):4781–4794. doi:10.1007/s12035-016-0021-1
53. Linke R, Pries R, Könnecke M, et al. The MEK1/2-ERK1/2 pathway is activated in chronic rhinosinusitis with nasal polyps. *Arch Immunol Ther Exp*. 2014;62(3):217–229. doi:10.1007/s00005-014-0281-2
54. Jiménez-Sousa MÁ, Martínez I, Medrano LM, Fernández-Rodríguez A, Resino S. Vitamin D in human immunodeficiency virus infection: influence on immunity and disease. *Front Immunol*. 2018;9:458. doi:10.3389/fimmu.2018.00458